A PI3Kγ mimetic peptide triggers CFTR gating, bronchodilation and reduced inflammation in obstructive airway diseases

Authors:
Alessandra Ghigo[1,2*†], Alessandra Murabito[1*], Valentina Sala[1,2], Anna Rita Pisano[3], Serena Bertolini[3], Ambra Gianotti[4], Emanuela Caci[4], Alessio Montresor[5,6], Aiswarya Premchandar[7], Flora Pirozzi[1,8], Kai Ren[1], Angela Della Sala[1], Marco Mergiotti[1], Wito Richter[9], Eyleen de Poel[10], Michaela Matthey[11], Sara Caldrer[5,6§], Rosa A. Cardone[12], Federica Civiletti[13], Andrea Costamagna[13], Nancy L. Quinney[14], Cosmin Butnarasu[1], Sonja Visentin[1], Maria Rosaria Ruggiero[1], Simona Baroni[1], Simonetta Geninatti Crich[1], Damien Ramel[15], Muriel Laffargue[15], Carlo G. Tocchetti[8,16,17], Renzo Levi[18], Marco Conti[19], Xiao-Yun Lu[20], Paola Melotti[21], Claudio Sorio[5,6], Virginia De Rose[1], Fabrizio Facchinetti[3], Vito Fanelli[13], Daniela Wenzel[11,22], Bernd K. Fleischmann[22], Marcus A. Mall[23,24], Jeffrey Beekman[10], Carlo Laudanna[5,6], Martina Gentzsch[14,25], Gergely L. Lukacs[7], Nicoletta Pedemonte[4], and Emilio Hirsch[1,2†]
*Equal contribution

Affiliations:
[1]Department of Molecular Biotechnology and Health Sciences, Molecular Biotechnology Center, University of Torino; 10126 Torino, Italy
[2]Kither Biotech S.r.l.; 10126 Torino, Italy
[3]Chiesi Farmaceutici S.p.A., Corporate Pre-Clinical R&D; 43122 Parma, Italy
[4]UOC Genetica Medica, IRCCS Istituto Giannina Gaslini; 16147 Genova, Italy
[5]Division of General Pathology, Department of Medicine, University of Verona School of Medicine; 37134 Verona, Italy
[6]Cystic Fibrosis Translational Research Laboratory "Daniele Lissandrini," Department of Medicine, University of Verona School of Medicine; 37134 Verona, Italy
[7]Department of Physiology, McGill University; H3G 1Y6 Montréal, Quebec, Canada
[8]Department of Translational Medical Sciences, Federico II University; 80131 Naples, Italy
[9]Department of Biochemistry & Molecular Biology, University of South Alabama College of Medicine; AL 36688 Mobile, Alabama, USA
[10]Department of Pediatric Pulmonology, Wilhelmina Children's Hospital, University Medical Center Utrecht; 3584 EA Utrecht, The Netherlands.
[11]Department of Systems Physiology, Medical Faculty, Ruhr University Bochum; 44801 Bochum, Germany
[12]Department of Biosciences, Biotechnologies and Biopharmaceutics, University of Bari; 70126 Bari, Italy
[13]Department of Anesthesia and Critical Care Medicine, University of Torino, Azienda Ospedaliera Città della Salute e della Scienza di Torino; 10126 Torino, Italy
[14]Marsico Lung Institute/Cystic Fibrosis Research Center, University of North Carolina; NC 27599 Chapel Hill, North Carolina, USA
[15]Institute of Metabolic and Cardiovascular Diseases, Paul Sabatier University; 31432 Toulouse, France
[16]Interdepartmental Center of Clinical and Translational Research (CIRCET), Federico II University; 80131 Naples, Italy

[17]Interdepartmental Hypertension Research Center (CIRIAPA), Federico II University; 80131 Naples, Italy

[18]Department of Life Sciences and Systems Biology, University of Torino, 10123 Torino, Italy

[19]Department of Obstetrics, Gynecology and Reproductive Sciences, University of California San Francisco; CA 94143 San Francisco, California, USA

[20]School of life Science & Technology, Xi'an Jiaotong University; 710049 Xi'an Shaanxi, P.R.China

[21]Cystic Fibrosis Center, Azienda Ospedaliera Universitaria Integrata di Verona; 37126 Verona, Italy

[22]Institute of Physiology I, Life & Brain Center, Medical Faculty, University of Bonn; 53127 Bonn, Germany

[23]Department of Pediatric Respiratory Medicine, Immunology and Critical Care Medicine, Charité-Universitätsmedizin Berlin; 10117 Berlin, Germany

[24]German Center for Lung Research (DZL), associated partner; 10117 Berlin, Germany

[25]Department of Pediatric Pulmonology, University of North Carolina; NC 27599 Chapel Hill, North Carolina, USA

§Actual position: Department of Infectious, Tropical Diseases and Microbiology, IRCCS Sacro Cuore Don Calabria Hospital; 37024 Negrar, Italy

Corresponding authors:

Alessandra Ghigo, alessandra.ghigo@unito.it; Emilio Hirsch, emilio.hirsch@unito.it.

One-sentence summary:
A PI3Kγ mimetic peptide enhances airway cAMP, dilates bronchi, reduces inflammation and promotes chloride secretion in obstructive airway diseases.

Editor's summary:

ABSTRACT

Cyclic adenosine 3',5'-monophosphate (cAMP) elevating agents, like β_2-adrenergic receptor (β_2-AR) agonists and phosphodiesterase (PDE) inhibitors, remain a mainstay in the treatment of obstructive respiratory diseases, conditions characterized by airway constriction, inflammation, and mucus hypersecretion. However, their clinical use is limited by unwanted side effects due to unrestricted cAMP elevation in the airways and in distant organs. Here we identified the A-kinase anchoring protein phosphoinositide 3-kinase γ (PI3Kγ) as a critical regulator of a discrete cAMP signaling microdomain activated by β_2-ARs in airway structural and inflammatory cells. Displacement of the PI3Kγ-anchored pool of protein kinase A (PKA) by an inhaled, cell-permeable, PI3Kγ mimetic peptide (PI3Kγ MP) inhibited a pool of subcortical PDE4B and PDE4D, and safely increased cAMP in the lungs, leading to airway smooth muscle relaxation and reduced neutrophil infiltration in a murine model of asthma. In human bronchial epithelial cells, PI3Kγ MP induced unexpected cAMP and PKA elevations restricted to the vicinity of the cystic fibrosis transmembrane conductance regulator (CFTR), the ion channel controlling mucus hydration that is mutated in cystic fibrosis (CF). PI3Kγ MP promoted the phosphorylation of wild-type CFTR on serine 737, triggering channel gating, and rescued the function of F508del-CFTR, the most prevalent CF mutant, by enhancing the effects of existing CFTR modulators. These results unveil PI3Kγ as the regulator of a β_2-AR/cAMP microdomain central to smooth muscle contraction, immune cell activation and epithelial fluid secretion in the airways, suggesting the use of a PI3Kγ MP for compartment-restricted, therapeutic cAMP elevation in chronic obstructive respiratory diseases.

INTRODUCTION

Obstructive airway diseases, including asthma, chronic obstructive pulmonary disease (COPD) and the genetic disorder cystic fibrosis (CF), represent a major health burden worldwide. Over the next decade, prevalence of asthma and COPD is predicted to rise in developing countries (*1*) and so is the number of CF patients requiring long-term care, because survival is progressively improving due to better treatments and intensive follow-up (*2*). Despite the diversity in etiology, pathogenetic mechanisms and clinical manifestations, these conditions share common features such as chronic airway inflammation, mucus hypersecretion and airflow obstruction due to airway hyperreactivity and/or mucus plugging (*1, 2*). Conventional medications, especially for asthma, include inhaled corticosteroids and β_2-adrenergic receptor (β_2-AR) agonists, which reduce airway inflammation and reverse airway constriction, respectively (*1*). Whereas the primary effect of β_2-AR agonists is relaxation of airway smooth muscle, these drugs can also engage this receptor in infiltrating leukocytes, eventually contributing to the resolution of inflammation through the cyclic adenosine 3',5'-monophosphate (cAMP) pathway (*3*). Furthermore, β_2 adrenergic receptors (β_2-AR) agonists are potent inducers of the cystic fibrosis transmembrane conductance regulator (CFTR) (*4*), the epithelial anion channel that drives airway surface fluid (ASL) hydration. CFTR dysfunction is a major cause of mucus hyper concentration that leads to impaired mucociliary clearance and mucus plugging in patients with the genetic disorder CF (*2*), but also in COPD (*5*) and asthma (*6*). Although β_2-AR agonists could be beneficial in these chronic obstructive diseases, their efficacy is still limited, primarily because of tachyphylaxis and adverse events, such as tachyarrhythmias, stemming from systemic drug exposure. Similarly, inhibition of cAMP breakdown by drugs targeting phosphodiesterase 4 (PDE4) (*7*), the major cAMP-hydrolyzing enzyme in the airways, is clinically effective but exhibits unwanted side effects, such as emesis, diarrhea, and weight loss, likely due to systemic PDE4 blockade (*8*). Thus, safer approaches for the manipulation of the β_2-AR/cAMP signaling axis for the treatment of chronic airway diseases are desirable.

Previous work from our group identified phosphoinositide 3-kinase γ (PI3Kγ) as a negative regulator of β_2-AR/cAMP signaling in the heart. In this tissue, PI3Kγ serves as an A-kinase anchoring protein (AKAP) that tethers protein kinase A (PKA) to PDE3 and PDE4, favoring their PKA-mediated phosphorylation and activation. This mechanism of localized PDE stimulation eventually allows restricting β_2-AR/cAMP responses to discrete subcellular compartments (*9, 10*). Accordingly, disruption of the scaffold but not the kinase activity of PI3Kγ results in β_2-AR/cAMP signaling amplification in cardiomyocytes (*9*). Because PI3Kγ is also found in pulmonary cells (*11*), we speculated that PI3Kγ could contribute to the compartmentalization of β_2-AR/cAMP responses in the lungs, and that pharmacological targeting of PI3Kγ scaffold activity could achieve therapeutic cAMP elevation in the airways.

Here, we described a cell-permeable PI3Kγ-derived mimetic peptide (PI3Kγ MP) that, by interrupting the interaction between PI3Kγ and PKA, inhibited PI3Kγ-associated PDE4B and PDE4D and, in turn, enhanced β_2-AR/cAMP responses in human bronchial smooth muscle, epithelial and immune cells. Intratracheal instillation of PI3Kγ MP limited bronchoconstriction and lung neutrophil infiltration in a mouse model of asthma. In human airway epithelial cells, PI3Kγ MP promoted gating of wild-type CFTR and restored the function of the most prevalent CFTR mutant in CF (F508del) by potentiating the effects of approved CFTR modulators.

RESULTS

A PI3Kγ mimetic peptide enhances airway β_2-AR/cAMP signaling

To assess the role of PI3Kγ scaffold activity in the regulation of airway cAMP, we compared PI3Kγ knock-out mice (PI3Kγ$^{-/-}$), lacking both the anchoring and the catalytic function of the p110γ subunit of PI3Kγ, with animals expressing a kinase-inactive p110γ that retains the scaffold activity (PI3Kγ kinase-dead, PI3Kγ$^{KD/KD}$) (*9*). The amount of cAMP was 2-fold higher in PI3Kγ$^{-/-}$ than in wild-type (PI3Kγ$^{+/+}$) and PI3Kγ$^{KD/KD}$ tracheas (Fig. 1A), suggesting a kinase-independent control of airway cAMP by PI3Kγ. Similar to previous findings in the heart (*9*), the increased cAMP concentration detected in PI3Kγ$^{-/-}$ tracheas correlated with reduced activity of PDE4B and PDE4D, while their function was normal in PI3Kγ$^{KD/KD}$ tissues (Fig. 1B). Modulation of PDE4B and PDE4D by PI3Kγ was also detected in isolated murine tracheal smooth muscle cells (mTSMCs) (Fig. 1C), where PI3Kγ was found to be highly abundant (Fig. 1D). As shown in Fig 1D, the canonical p110γ doublet was detectable in PBMCs and tracheas, whereas mTSMCs and hBSMCs displayed the low molecular weight isoform only. These PI3Kγ forms were found to organize multiprotein-complexes containing both PDEs and their activator PKA (Fig. 1, E and F). Downregulation of the *PIK3CG* gene (encoding p110γ) in human bronchial smooth muscle cells (hBSMCs) increased β$_2$-AR-activated cAMP responses by 30% (Fig. 1G), thus supporting a PI3Kγ kinase-independent activation of PDE4, restraining airway cAMP downstream of β$_2$-ARs. These findings prompted us to design a molecule interfering with the scaffold function of PI3Kγ and enhancing β$_2$-AR/cAMP signaling in the airways. To disrupt the PKA-anchoring function of PI3Kγ in vivo, a peptide encompassing the PKA-binding motif of PI3Kγ (*10*) was fused to the cell-penetrating sequence penetratin-1 (P1) (*12*) (Fig. 2A). A fluorescein isothiocyanate (FITC)-labeled version of this PI3Kγ mimetic peptide (PI3Kγ MP) was detectable in hBSMCs within 30 min of administration (Fig. 2A). PI3Kγ MP associated the recombinant RIIα subunit of PKA with a dissociation constant of 7.5 µM (Fig. 2B) and dose-dependently disrupted the PKA-RII/p110γ interaction (Fig. 2C). Conversely, PI3Kγ MP did not alter C5a-mediated Akt phosphorylation (Fig. S1A), indicating that it did not interfere with the kinase function of PI3Kγ (*9*). In line with the ability to disturb PKA/p110γ association, PI3Kγ MP reduced PDE4B and PDE4D activity by 30% in primary wild-type mTSMCs, whereas no significant effect of the peptide was observed in PI3Kγ-deficient cells (*P*>0.9999)(Fig. 2D). Similarly, PI3Kγ MP failed to increase cAMP in PI3Kγ$^{-/-}$ macrophages (Fig. S1B), confirming that PI3Kγ MP specifically inhibited PI3Kγ-associated PDEs but not PDEs anchored to other AKAPs (*7*). In hBSMCs, PI3Kγ MP, but not a control peptide (CP) containing penetratin-1 only, increased β$_2$-AR-evoked cAMP responses by 35% (Fig. 2E). Furthermore, PI3Kγ MP induced cAMP elevation in human airway epithelial cells (16HBE14o-) with a maximal effective concentration of 21.66 µM (Fig. 2F), whereas a control peptide containing penetratin-1 fused to a scrambled sequence of the PKA-binding site of p110γ failed to affect cAMP abundance (Fig. S1C).

To assess whether PI3Kγ MP could enhance airway β$_2$-AR/cAMP signaling in vivo, the peptide was instilled intratracheally in mice and found to induce a dose-dependent increase in cAMP, with 80 µg/kg as the lowest dose eliciting a significant increase in cAMP concentration in both tracheas (*P*<0.0001) and lungs (*P*=0.0288) (Fig. 3A). Mice receiving 80 µg/kg of FITC-labeled PI3Kγ MP showed fluorescence in the airways as soon as 30 min after a single intratracheal administration (Fig. S2A), when the amount of cAMP was already 30% higher than in tissues from animals receiving either saline or CP (Fig. S2B). Moreover, PI3Kγ MP persisted in the airways up to 24 hours after a single-dose instillation (Fig. 3B), when maximal cAMP accumulation was detected (Fig. 3C). Notably, direct intrapulmonary application prevented PI3Kγ MP from diffusing outside of the respiratory tract as well as from altering cAMP

homeostasis in the heart (Fig. 3, A to C). No systemic side effects were observed after chronic exposure to PI3Kγ MP, as evidenced by histopathological examination of major organs (Fig. S3A), body weight monitoring (Fig. S3B), blood biochemical tests and cardiac function analysis (Tables S1 and S2). Furthermore, negligible immunogenicity was observed only after repeated systemic administration of the peptide in the presence of adjuvants (Fig. S3C), whereas PI3Kγ MP did not elicit any antibody response when applied locally (Fig. S3D). Thus, inhalation of PI3Kγ MP might be safely employed to boost airway $β_2$-AR/cAMP signaling in vivo.

PI3Kγ MP induces airway relaxation in a mouse model of asthma
Next, we assessed ex-vivo in mouse tracheal rings if the PI3Kγ scaffold activity affected cAMP-dependent airway smooth muscle relaxation. Acetylcholine-induced contraction was lower in $PI3Kγ^{-/-}$ tracheas than in $PI3Kγ^{+/+}$ controls, while $PI3Kγ^{KD/KD}$ rings exhibited normal tone (Fig. 4A). Similarly, carbachol-dependent contractility was 35% lower in $PI3Kγ^{-/-}$ than in $PI3Kγ^{+/+}$ and $PI3Kγ^{KD/KD}$ samples (Fig. 4B). Next, $PI3Kγ^{+/+}$ and $PI3Kγ^{-/-}$ rings were pre-treated with the selective PDE4 inhibitor roflumilast before exposure to carbachol. PDE4 inhibition decreased the contraction of $PI3Kγ^{+/+}$ rings to the values observed in $PI3Kγ^{-/-}$ samples, where the inhibitor was ineffective (Fig. 4C), thus confirming that the decreased contraction of $PI3Kγ^{-/-}$ airways is causally linked to a reduction in PDE4 activity.
We then determined whether PI3Kγ MP could phenocopy the reduced contractility observed in $PI3Kγ^{-/-}$ airways. Lung resistance was assessed in healthy wild-type mice pre-treated with an aerosol of PI3Kγ MP, CP, or saline, before exposure to increasing doses of the contracting agent methacholine (MCh). MCh triggered a dose-dependent increase in airway resistance that was lower in mice treated with PI3Kγ MP than in animals exposed to CP (Fig. 4D). Next, we tested the ability of the peptide to promote airway relaxation in ovalbumin (OVA)-sensitized mice, a well-established model of asthma. Single-dose inhalation of PI3Kγ MP significantly increased the amount of cAMP in lungs ($P=0.0065$) and tracheas ($P=0.0137$) (Fig. 4E) and reduced MCh-induced bronchoconstriction, as evidenced by measurements of both tidal volume (Fig. 4F) and lung resistance (Fig. 4G). Thus, PI3Kγ MP could alleviate bronchoconstriction associated with asthma via elevation of cAMP.

PI3Kγ MP limits neutrophilic inflammation in a mouse model of asthma
Because cAMP-elevating agents have anti-inflammatory actions (3), we tested whether PI3Kγ MP could relieve airway inflammation in OVA-sensitized mice. Peribronchial inflammation and mucin production were dampened in animals repeatedly exposed to PI3Kγ MP (Fig. 5, A and B). Moreover, a significantly lower number of neutrophils was detected in the BAL fluid of PI3Kγ MP-treated mice than in controls ($P=0.0437$) (Fig. 5C), indicating that PI3Kγ MP inhibits the neutrophilic inflammation associated with asthma. PI3Kγ MP also inhibited chemoattractant-induced adhesion of human neutrophils to ICAM-1 and ICAM-2 (Fig. S4, A and B) by reducing LFA-1 activation (Fig. S4C). PKA inhibition rescued neutrophil adhesion to ICAM-1, ICAM-2, and fibrinogen (Fig. 5, D to F) in the presence of PI3Kγ MP, indicating that the impaired adhesion was dependent on PKA hyperactivation. In line with ICAM-1 controlling neutrophil recruitment to the airways, PI3Kγ MP significantly reduced neutrophil chemotaxis to fMLP ($P<0.0001$) via PKA activation (Fig. 5G) and the consequent inhibition of RhoA-mediated (Fig. 5H) LFA-1 triggering (13). Thus, PI3Kγ MP could limit neutrophilic inflammation in asthma by dampening neutrophil adhesion and transmigration.

PI3Kγ MP promotes cAMP-dependent activation of CFTR and chloride efflux in airway epithelial cells

Next, we tested whether PI3Kγ MP could promote chloride (Cl⁻) secretion via the cAMP-gated CFTR channel. PI3Kγ was enriched at the apical membrane of 16HBE14o- cells (Fig. S5A) and coimmunoprecipitated with CFTR (Fig. S5B). Fluorescence resonance energy transfer (FRET) analysis showed that, in response to forskolin (Fsk), PI3Kγ MP induced 3-fold higher subcortical membrane cAMP concentration than either CP or saline (Fig. 6A), while not affecting cytosolic cAMP responses (Fig. 6A).

To test if PI3Kγ MP could trigger CFTR gating, PKA-mediated phosphorylation of the channel was assessed by Western blot and found to be 5-fold higher in 16HBE14o- cells treated with PI3Kγ MP than in cells exposed to either vehicle or CP (Fig. 6B). PI3Kγ MP increased CFTR phosphorylation to a similar extent as rolipram, implying that PI3Kγ MP impacts on PDE4-mediated regulation of CFTR (*14*). To further characterize the CFTR phosphorylation elicited by PI3Kγ MP, the phospho-occupancy of known PKA sites in the regulatory domain of the channel was analyzed by liquid chromatography-coupled tandem mass spectrometry in cystic fibrosis human bronchial epithelial cells expressing a wild-type CFTR (wt-CFTR-CFBE41o-) (*15*), treated with either PI3Kγ MP, CP, Fsk or vehicle. While Fsk-mediated adenylyl cyclase activation triggered the phosphorylation of most PKA sites, PI3Kγ MP selectively increased the phospho-occupancy of S737 and, to a lesser extent, of S753 (Fig. 6C and Fig. S6, A to C). In agreement with mass spectrometry results, the CFTR phosphorylation elicited by PI3Kγ MP was completely abolished in cells expressing a CFTR mutant where the serine was replaced by alanine (Fig. 6D).

Because phosphorylation of S737 can lead to a ~25% increase in the open probability of CFTR (*16*), we anticipated that PI3Kγ MP could activate Cl⁻ secretion. Measurement of short-circuit currents (I_{SC}) showed that acute application of PI3Kγ MP to polarized wt-CFTR-CFBE41o-monolayers induced a dose-dependent increase in CFTR conductance (Fig. S7A), reaching up to either 30% or 45% of the maximal channel activation, when applied either alone or in association with nanomolar doses of Fsk, respectively (Fig. S7, A to C). Addition of the adenylate cyclase inhibitor SQ22536 and the PKA blocker H89 after treatment with PI3Kγ MP inhibited the increase in CFTR conductance elicited by the peptide (Fig. S7D), confirming that PI3Kγ MP activated CFTR through PKA.

I_{SC} measurements in primary human bronchial epithelial (HBE) cells showed that PI3Kγ MP, but not CP, induced a dose-dependent increase in CFTR currents (Fig. 6E). No further elevation in I_{SC} was observed when rolipram was added to PI3Kγ MP (Fig. 6E), confirming that the peptide inhibited the PDE4 pool associated to CFTR regulation (*14*). Boosting cAMP production with Fsk produced an additional increment of I_{SC} that was blocked by the CFTR inhibitor 172 (CFTR$_{inh}$-172) (Fig. 6E). Similarly, the non-hydrolysable cAMP analog CPT-cAMP further increased I_{SC} in addition to PI3Kγ MP (Fig. S8, A and B), but blocked the effect of the peptide on CFTR currents when applied as a pre-treatment (Fig. S8A, to C), providing further evidence that PI3Kγ MP activated the channel through cAMP and PKA.

Primary HBE cells express other cAMP/PKA-dependent ion channels and transporters that can indirectly influence CFTR activity by increasing the electrochemical driving force (*17*). In the presence of CFTR$_{inh}$-172, PI3Kγ MP retained the ability to induce a transient increase in I_{SC} (Fig. S8D) indicating the opening of Ca²⁺-activated Cl⁻ channels (CaCCs). Furthermore, the current

decreased to baseline after application of clotrimazole (Fig. S8D), an inhibitor of basolateral Ca^{2+}-activated K^+ channels, and bumetanide, an inhibitor of the Na-K-Cl cotransporter NKCC1 (Fig. S8D), suggesting that the peptide could also promote luminal Cl^- secretion indirectly via these channels. To further evaluate the direct action of PI3Kγ MP on CFTR currents, Ca^{2+} stores were first depleted with thapsigargin (Fig. S8, E and F) and then CaCCs were blocked using either a general CaCC inhibitor (Fig. S8E) or an inhibitor targeting TMEM16A (Fig. S8F), the major CaCC isoform in HBE cells. Without functional CaCCs, PI3Kγ MP elicited a response that was fully abolished by CFTR$_{inh}$-172, confirming a direct activation of CFTR (Fig. S8E). This observation was corroborated in rectal organoids, where CaCCs are not consistently expressed, and organoid swelling in response to Fsk (FIS) is CFTR-dependent (*18*). PI3Kγ MP potentiated by 2-fold the swelling of wild-type organoids elicited by a low dose of Fsk (2 µM) priming cAMP production (Fig. 6F). As CFTR activation triggers water secretion, essential for proper mucus hydration and clearance (*2*), PI3Kγ MP, but not CP, decreased intracellular water residence time, indicative of rapid water efflux, in cells expressing wt-CFTR (Fig. 6G). Hence, PI3Kγ MP could induce Cl^- and consequent water secretion in bronchial epithelial cells through a cAMP-dependent mechanism, coordinating direct CFTR gating with the elevation of the electrochemical driving force.

PI3Kγ MP enhances the therapeutic effects of CFTR modulators in cystic fibrosis in vitro models

Next, we tested if PI3Kγ MP could rescue the function of the most common CF-causing CFTR mutant (F508del-CFTR). F508del-CFTR exhibits multiple molecular defects that require the combined use of correctors (VX-809/lumacaftor, VX-661/tezacaftor or VX-445/elexacaftor) and a potentiator (VX-770/ivacaftor) to restore the plasma membrane localization and channel gating, respectively (*2*). In the presence of the corrector VX-809, PI3Kγ MP enhanced subcortical cAMP concentrations by 35% in F508del-CFTR-CFBE41o- cells (Fig. 7A). Furthermore, primary HBE cells from a patient homozygous for the F508del mutation, treated with the first-generation combination of VX-809 and VX-770, showed a 5-fold increase in I$_{SC}$ when PI3Kγ MP was given after acute administration of VX-770 (Fig. 7B). Similar results were obtained in F508del/F508del HBE cells from a second donor, with the exception that in these cells PI3Kγ MP, added in addition to VX-770, stimulated a biphasic response, with a first I$_{SC}$ peak that indicated CaCC activation, followed by a plateau phase corresponding to CFTR$_{inh}$-172-sensitive CFTR-mediated currents (Fig. 7C and Fig. S9, A to D). In agreement with a coordinated action of the peptide on CFTR currents and the electrochemical driving force, I$_{SC}$ was completely abolished by sequential application of CFTR$_{inh}$-172, clotrimazole and bumetanide (Fig. S9, A to C). The synergy between the CFTR potentiator VX-770 and PI3Kγ MP was further supported by FIS assays in intestinal organoids. The effect of the peptide was first assessed in organoids derived from compound heterozygotes bearing the F508del allele and the residual function mutation D1152H. After correction with VX-809, organoid size was increased by 50% in the group pre-treated with PI3Kγ MP before stimulation with VX-770 and Fsk (Fig. 7D), and CFTR$_{inh}$-172 prevented this effect (Fig. 7D). In F508del/F508del organoids under chronic treatment with VX-809 and VX-770, where their interaction reduces correction efficacy (*19*), PI3Kγ MP dose-dependently increased organoid size up to 6.5-fold the volume of controls (Fig. 7E). The maximal synergy between the peptide and CFTR modulators was observed at a low non-saturating dose of Fsk (0.051 µM), which was expected to minimally

increase the amount of cAMP, and which was almost ineffective in inducing swelling in the control VX-770+VX-809 group.

Last, we assessed the ability of PI3Kγ MP to enhance the therapeutic effects of the recent triple combination elexacaftor/tezacaftor/ivacaftor (VX-445+VX-661+VX-770) in F508del/F508del HBE cells from two different donors with CF. VX-770-mediated Cl$^-$ currents were 40% higher in cells treated chronically with VX-661+VX-445 together with PI3Kγ MP than in controls exposed to correctors alone (Fig. 8, A to C and Fig. S9E). In both cases, CPT-cAMP further increased Cl$^-$ currents, which were inhibited by CFTR$_{inh}$-172, further demonstrating that Cl$^-$ secretion was CFTR-dependent. These data thus suggest the use of PI3Kγ MP to increase the efficacy of CFTR modulators as well as to provide bronchodilator and anti-inflammatory activities, potentially beneficial to CF and other diseases like COPD and asthma.

DISCUSSION

Our results establish that targeting the PKA-anchoring function of PI3Kγ with a mimetic peptide allows therapeutic manipulation of β$_2$-AR/cAMP signaling in multiple cell types participating to the pathogenesis of chronic obstructive airway diseases (Fig. S10). These findings are consistent with a model where PI3Kγ acts as a scaffold protein for PKA (AKAP) in a complex containing the PKA-dependent phosphodiesterase PDE4 (7). The pharmacological actions of PI3Kγ MP stem from its ability to displace PKA from the PI3Kγ complex, thereby preventing PKA-mediated stimulation of a pool of PDE4 that is responsible for lowering the amount of cAMP close to neighboring distinct PKA-containing complexes, including those regulating CFTR gating (14).

Our finding that PI3Kγ MP fails to increase cAMP in PI3Kγ-deficient cells demonstrates that the peptide inhibits uniquely PI3Kγ-dependent PDEs and does so without disturbing other AKAP-PKA complexes. This is supported by our previous findings showing that the PKA-binding sequence of the peptide diverges from that of classical AKAPs (10).

Although the AKAP function of PI3Kγ has been previously linked to cAMP modulation in the heart (9, 10) and in vascular smooth muscles (20), the role and the pathophysiological relevance of PI3Kγ non-catalytic activity outside the cardiovascular system has remained elusive. The present study identified the scaffold function of PI3Kγ as a key negative regulator of a discrete cAMP/PKA microdomain in different cell subsets of the airways, including epithelial, smooth muscle and immune cells. Like in cardiomyocytes (9), in airway cells PI3Kγ-mediated reduction of cAMP is spatially confined to compartments that contain β$_2$-ARs, key pharmacological targets for respiratory diseases. Although the effects of PI3Kγ MP might be attained with the use of β$_2$-AR agonists, these drugs suffer from efficacy and tolerability concerns, linked to tachyphylaxis and unwanted pharmacological effects outside the lungs. Unlike β$_2$-AR agonists, PI3Kγ MP acts through a distinct mechanism with at least two advantages. First, PI3Kγ MP amplifies β$_2$-AR/cAMP responses by impinging on cAMP degradation rather than on β$_2$-AR activation, thus avoiding receptor desensitization that, in the long run, is a major cause of reduced efficacy. Second, being an inhaled peptide of 5 KDa, PI3Kγ MP boosts lung cAMP without reaching other tissues where cAMP elevation would not be desirable, such as in the heart (9).

In addition, the local action of the peptide provides an added value over other cAMP-elevating agents, such as the classical small molecule PDE4 inhibitors, like roflumilast, that easily diffuse outside the lungs and trigger undesired brain and cardiac effects (8). In addition, small molecule PDE4 inhibitors lead to indiscriminate inhibition of all four different PDE4 subtypes (PDE4A, B,

C and D), potentially causing further side effects. Intriguingly, PI3Kγ MP blocked selective PDE4 subtypes with a prominent role in the lungs, such as PDE4B and PDE4D (*21*), with high isoform and compartment selectivity.

Consistent with the pro-relaxing action of cAMP, PI3Kγ MP demonstrated prominent bronchodilator effects in vivo in healthy and asthmatic mice, which could be explained by enhanced $β_2$-AR/cAMP signaling, secondary to PDE4 inhibition in airway smooth muscle cells. Although the broncho-relaxant action of $β_2$-AR agonists, such as salbutamol and formoterol, is well established, conflicting findings have been reported for PDE4 inhibitors (*21*). Our observation that roflumilast blunts PI3Kγ-dependent contractility of tracheal rings confirms a role for PDE4 in regulating airway smooth muscle tone. This view agrees with previous reports of reduced airway smooth muscle contractility in *Pde4d* knock-out mice (*22*) and of enhanced $β_2$-AR-stimulated cAMP accumulation in *PDE4D5* knockdown human smooth muscle cells (*23*). PDE4 is also enriched in immune cells, and PDE4 inhibitors have demonstrated anti-inflammatory properties (*7, 21*). The finding that PI3Kγ MP specifically inhibited neutrophil recruitment suggests that this peptide might be effective in hard-to-treat chronic airway disease subtypes with neutrophilic inflammation, such as corticosteroid-insensitive neutrophilic asthma (*24*), as well as COPD and CF (*2, 25*). Similar to standard anti-inflammatory drugs, such as inhaled corticosteroids, PI3Kγ MP might increase the risk of respiratory infections, requiring antibiotic therapy. This is particularly relevant to CF patients who already suffer from infections causing lung function decline and, ultimately, mortality (*2*). A limitation of our study is that the effects of PI3Kγ MP were not tested in infection models. Hence, although genetic and pharmacologic PDE4 inhibition appear safe in pulmonary infections (*26*), future studies are required to define whether PI3Kγ MP affects host defense.

Another effect of targeting PDE4 is the cAMP/PKA-dependent gating of the CFTR channel, increasing airway surface liquid and facilitating mucus clearance (*27*). CFTR functional defects and mucus stasis can be observed in patients with COPD and certain forms of asthma (*28*) but are critical in CF (*2*). Previous reports identified PDE4D as a negative regulator of the cAMP/PKA-dependent activation of wild-type CFTR in bronchial epithelial cells, highlighting the potential of PDE4 inhibitors to stimulate the channel (*14, 29*). Our study pinpoints PI3Kγ as a key AKAP orchestrating cAMP-mediated signal transduction in a microdomain involving $β_2$-ARs, PDE4D, and CFTR. Accordingly, whereas a generalized cAMP elevation induced by forskolin correlated with the phosphorylation of most of CFTR phospho-sites, PI3Kγ MP triggered local cAMP elevation, resulting in the selective phosphorylation of S737. Although S737 phosphorylation might have contrasting effects on CFTR gating (*16, 30*), this likely depends on contextual modifications of other phosphorylation sites (*31*) and our observations indicate that PI3Kγ MP-mediated phosphorylation of S737 triggers the same activity observed after reintroduction of S737 in a PKA-insensitive CFTR mutant (*16*). Intriguingly, PI3Kγ MP contributes to Cl⁻ secretion not only through a direct action on CFTR, but also by engaging Ca^{2+}-activated Cl⁻ channels and basolateral, clotrimazole-sensitive Ca^{2+}-activated K^+ channels increasing the electrochemical driving force (*17*). Hence, PI3Kγ MP coordinates different mechanisms culminating in Cl⁻ secretion, provided that sufficient functional CFTR is appropriately located at the plasma membrane.

In CF, the most common CFTR mutation (F508del) leads to the intracellular retention of the channel (*2*). The function of F508del-CFTR can be improved by the combined administration of correctors and potentiators, that enable the plasma membrane exposure and facilitate PKA-dependent gating of the mutant channel, respectively (*2, 32*). In agreement, the efficacy of the

potentiator VX-770 depends on concomitant cAMP/PKA phosphorylation of the channel (*33*). Although forskolin has been extensively used to elevate cAMP in the preclinical testing of all CFTR modulators, PI3Kγ MP ensured a more physiological and compartment-restricted increase in cAMP in the vicinity of CFTR that maximized the action of all combinations, including both lumacaftor/ivacaftor and elexacaftor/tezacaftor/ivacaftor (ETI). Despite the improvement in lung function achieved with ETI (*2*), rescue of CFTR activity does not reach more than 60% of physiological values (*34, 35*). Our observation that the peptide can almost double the gating of the F508del-CFTR mutant after correction and potentiation with ETI suggests that enhancing PKA-mediated CFTR phosphorylation might represent an avenue for reinstating F508del-CFTR activity close to 100% of wild-type function, a condition potentially matching that of healthy carriers of CF mutations (*34*). Our initial preclinical toxicology studies in mice have shown that the inhaled PI3Kγ MP remains confined in the lungs and is tolerable, but additional investigations in other animal models are awaited to corroborate the ability of the aerosolized peptide to overcome the mucus barrier imposed by CF (*36*). Nonetheless, treatment with ETI is associated with a substantial improvement in mucus mobilization (*37*) and could thus facilitate the combined action of PI3Kγ MP.

Taken together, this study highlights the therapeutic potential of increasing cAMP concentrations in a compartmentalized manner. With its pharmacological properties, PI3Kγ MP might be useful for the treatment of airway diseases including asthma and COPD, where cAMP-elevating agents with broncho-relaxant properties are highly desirable. In addition, by inhibiting PDE4, PI3Kγ MP may exert a selective activity on neutrophil adhesion and pulmonary recruitment. Finally, PI3Kγ MP might be used in CF where, despite the success of currently approved modulators, treatments allowing patients a normal lifespan are still lacking.

MATERIALS AND METHODS

Study Design. We tested the hypothesis that targeting the scaffold function of PI3Kγ could trigger local cAMP elevation in the lungs and could reduce airway smooth constriction, pulmonary inflammation, and mucus stasis in chronic respiratory diseases, without incurring unwanted systemic side effects. We devised a cell-penetrating peptide disturbing the AKAP function of PI3Kγ (PI3Kγ MP) and we tested its ability to induce compartmentalized cAMP responses in vitro in human bronchial smooth muscle (hBSMCs) and epithelial (16HBE14o−) cells, as well as in vivo after intratracheal instillation in mice. Bronchodilator and anti-inflammatory activities of PI3Kγ MP were studied in vivo in a mouse model of asthma (OVA-sensitized mice). Effects on CFTR activity were studied in primary human bronchial epithelial cells and intestinal organoids from healthy controls and donors with CF, through I_{sc} measurements and forskolin-induced swelling (FIS) assays, respectively.

The sample size for each experiment is included in the figure legends. For mouse studies, females and males of 8–12 weeks of age were used and randomly assigned to the experimental groups. Experiments were approved by the animal ethical committee of the University of Torino and by the Italian Ministry of Health (Authorization n°757/2016-PR). The number of mice in each group was determined by power calculations based on previous experience with the model system and is defined in the respective figure legends. For in vitro experiments using immortalized cell lines, at least 3 independent experiments were performed. For in vitro studies in cells and organoids derived from human subjects, the results of at least n=2 independent cultures from n=2 different donors are provided. Informed consent was obtained from all participating subjects and all studies were ethically approved. All experiments were conducted by blinded researchers. When outliers were identified, they were excluded from analysis if justified based on confirmed technical failure in parameter acquisition. Further details can be found in relevant sections within the Supplementary Materials and Methods.

Animals. PI3Kγ-deficient mice (PI3Kγ$^{-/-}$) and knock-in mice with catalytically inactive PI3Kγ (PI3Kγ$^{KD/KD}$) were described previously (*38, 39*). Mutant mice were back-crossed with C57Bl/6j mice for 15 generations to inbreed the genetic background and C57Bl/6j were used as controls (PI3Kγ$^{+/+}$). For asthma studies, wild-type BALB/C females were used. Mice used in all experiments were 8–12 weeks of age. Mice were group-housed, provided free-access to standard chow and water in a controlled facility providing a 12-hour light/dark cycle and were used according to institutional animal welfare guidelines and legislation, approved by the local Animal Ethics Committee. All animal experiments were approved by the animal ethical committee of the University of Torino and by the Italian Ministry of Health (Authorization n°757/2016-PR).

Human material. Approval for primary bronchial epithelial cells and organoids cultures was obtained by the different local ethics committees (University of California San Francisco, Istituto Giannina Gaslini, the University of North Carolina at Chapel Hill, University of Verona and University Medical Center Utrecht) and informed consent was obtained from all participating subjects.

Statistical analysis. Prism software (GraphPad software Inc) was used for statistical analysis. Data are presented as scatter plots with bars [means ± standard error of the mean (SEM)]. Raw data were first analyzed to confirm their normal distribution via the Shapiro-Wilk test and then analyzed by unpaired Student's *t* test, one-way analysis of variance (ANOVA) or two-way ANOVA. Bonferroni correction (one-way and two-way ANOVA) was applied to correct for multiple comparisons. In the absence of a normal distribution, nonparametric Kruskal-Wallis or Mann-Whitney tests were used, followed by Dunn's correction for multiple comparisons if appropriate. *P*<0.05 was considered significant.

SUPPLEMENTARY MATERIALS
Materials and Methods
Fig. S1 to S10.
Table S1 and S2.
Data File S1 and S2
References (*38-60*)

REFERENCES

1. B. R. Celli, J. A. Wedzicha, Update on Clinical Aspects of Chronic Obstructive Pulmonary Disease. *N Engl J Med* **381**, 1257-1266 (2019).
2. M. Shteinberg, I. J. Haq, D. Polineni, J. C. Davies, Cystic fibrosis. *Lancet* **397**, 2195-2211 (2021).
3. P. J. Barnes, New drugs for asthma. *Nat Rev Drug Discov* **3**, 831-844 (2004).
4. L. A. Vijftigschild, G. Berkers, J. F. Dekkers, D. D. Zomer-van Ommen, E. Matthes, E. Kruisselbrink, A. Vonk, C. E. Hensen, S. Heida-Michel, M. Geerdink, H. M. Janssens, E. A. van de Graaf, I. Bronsveld, K. M. de Winter-de Groot, C. J. Majoor, H. G. Heijerman, H. R. de Jonge, J. W. Hanrahan, C. K. van der Ent, J. M. Beekman, beta2-Adrenergic receptor agonists activate CFTR in intestinal organoids and subjects with cystic fibrosis. *Eur Respir J* **48**, 768-779 (2016).
5. E. M. Dunican, B. M. Elicker, T. Henry, D. S. Gierada, M. L. Schiebler, W. Anderson, I. Barjaktarevic, R. G. Barr, E. R. Bleecker, R. C. Boucher, R. Bowler, S. A. Christenson, A. Comellas, C. B. Cooper, D. Couper, G. J. Criner, M. Dransfield, C. M. Doerschuk, M. B. Drummond, N. N. Hansel, M. K. Han, A. T. Hastie, E. A. Hoffman, J. A. Krishnan, S. C. Lazarus, F. J. Martinez, C. E. McCulloch, W. K. O'Neal, V. E. Ortega, R. Paine, 3rd, S. Peters, J. D. Schroeder, P. G. Woodruff, J. V. Fahy, Mucus Plugs and Emphysema in the Pathophysiology of Airflow Obstruction and Hypoxemia in Smokers. *Am J Respir Crit Care Med* **203**, 957-968 (2021).

6.   E. M. Dunican, B. M. Elicker, D. S. Gierada, S. K. Nagle, M. L. Schiebler, J. D. Newell, W. W. Raymond, M. E. Lachowicz-Scroggins, S. Di Maio, E. A. Hoffman, M. Castro, S. B. Fain, N. N. Jarjour, E. Israel, B. D. Levy, S. C. Erzurum, S. E. Wenzel, D. A. Meyers, E. R. Bleecker, B. R. Phillips, D. T. Mauger, E. D. Gordon, P. G. Woodruff, M. C. Peters, J. V. Fahy, L. National Heart, P. Blood Institute Severe Asthma Research, Mucus plugs in patients with asthma linked to eosinophilia and airflow obstruction. *J Clin Invest* **128**, 997-1009 (2018).

7.   D. H. Maurice, H. Ke, F. Ahmad, Y. Wang, J. Chung, V. C. Manganiello, Advances in targeting cyclic nucleotide phosphodiesterases. *Nat Rev Drug Discov* **13**, 290-314 (2014).

8.   Y. Oba, Phosphodiesterase inhibitors in chronic obstructive pulmonary disease. *Am J Respir Crit Care Med* **188**, 1366 (2013).

9.   A. Ghigo, A. Perino, H. Mehel, A. Zahradnikova, Jr., F. Morello, J. Leroy, V. O. Nikolaev, F. Damilano, J. Cimino, E. De Luca, W. Richter, R. Westenbroek, W. A. Catterall, J. Zhang, C. Yan, M. Conti, A. M. Gomez, G. Vandecasteele, E. Hirsch, R. Fischmeister, Phosphoinositide 3-kinase gamma protects against catecholamine-induced ventricular arrhythmia through protein kinase A-mediated regulation of distinct phosphodiesterases. *Circulation* **126**, 2073-2083 (2012).

10.   A. Perino, A. Ghigo, E. Ferrero, F. Morello, G. Santulli, G. S. Baillie, F. Damilano, A. J. Dunlop, C. Pawson, R. Walser, R. Levi, F. Altruda, L. Silengo, L. K. Langeberg, G. Neubauer, S. Heymans, G. Lembo, M. P. Wymann, R. Wetzker, M. D. Houslay, G. Iaccarino, J. D. Scott, E. Hirsch, Integrating cardiac PIP3 and cAMP signaling through a PKA anchoring function of p110gamma. *Mol Cell* **42**, 84-95 (2011).

11.   V. Fanelli, V. Puntorieri, B. Assenzio, E. L. Martin, V. Elia, M. Bosco, L. Delsedime, L. Del Sorbo, A. Ferrari, S. Italiano, A. Ghigo, A. S. Slutsky, E. Hirsch, V. M. Ranieri, Pulmonary-derived phosphoinositide 3-kinase gamma (PI3Kgamma) contributes to ventilator-induced lung injury and edema. *Intensive Care Med* **36**, 1935-1945 (2010).

12.   G. Guidotti, L. Brambilla, D. Rossi, Cell-Penetrating Peptides: From Basic Research to Clinics. *Trends Pharmacol Sci* **38**, 406-424 (2017).

13.   C. Laudanna, J. J. Campbell, E. C. Butcher, Elevation of intracellular cAMP inhibits RhoA activation and integrin-dependent leukocyte adhesion induced by chemoattractants. *J Biol Chem* **272**, 24141-24144 (1997).

14.   E. Blanchard, L. Zlock, A. Lao, D. Mika, W. Namkung, M. Xie, C. Scheitrum, D. C. Gruenert, A. S. Verkman, W. E. Finkbeiner, M. Conti, W. Richter, Anchored PDE4 regulates chloride conductance in wild-type and DeltaF508-CFTR human airway epithelia. *FASEB J* **28**, 791-801 (2014).

15.   A. Schnur, A. Premchandar, M. Bagdany, G. L. Lukacs, Phosphorylation-dependent modulation of CFTR macromolecular signalling complex activity by cigarette smoke condensate in airway epithelia. *Sci Rep* **9**, 12706 (2019).

16.   T. Hegedus, A. Aleksandrov, A. Mengos, L. Cui, T. J. Jensen, J. R. Riordan, Role of individual R domain phosphorylation sites in CFTR regulation by protein kinase A. *Biochim Biophys Acta* **1788**, 1341-1349 (2009).

17.   S. L. Martin, V. Saint-Criq, T. C. Hwang, L. Csanady, Ion channels as targets to treat cystic fibrosis lung disease. *J Cyst Fibros* **17**, S22-S27 (2018).

18.   J. F. Dekkers, C. L. Wiegerinck, H. R. de Jonge, I. Bronsveld, H. M. Janssens, K. M. de Winter-de Groot, A. M. Brandsma, N. W. de Jong, M. J. Bijvelds, B. J. Scholte, E. E. Nieuwenhuis, S. van den Brink, H. Clevers, C. K. van der Ent, S. Middendorp, J. M. Beekman, A functional CFTR assay using primary cystic fibrosis intestinal organoids. *Nat Med* **19**, 939-945 (2013).

19.   D. M. Cholon, N. L. Quinney, M. L. Fulcher, C. R. Esther, Jr., J. Das, N. V. Dokholyan, S. H. Randell, R. C. Boucher, M. Gentzsch, Potentiator ivacaftor abrogates pharmacological correction of DeltaF508 CFTR in cystic fibrosis. *Sci Transl Med* **6**, 246ra296 (2014).

20.   A. Lupieri, R. Blaise, A. Ghigo, N. Smirnova, M. K. Sarthou, N. Malet, I. Limon, P. Vincent, E. Hirsch, S. Gayral, D. Ramel, M. Laffargue, A non-catalytic function of PI3Kgamma drives smooth muscle cell proliferation after arterial damage. *J Cell Sci* **133**, (2020).

21.   H. Zuo, I. Cattani-Cavalieri, N. Musheshe, V. O. Nikolaev, M. Schmidt, Phosphodiesterases as therapeutic targets for respiratory diseases. *Pharmacol Ther* **197**, 225-242 (2019).
22.   C. Mehats, S. L. Jin, J. Wahlstrom, E. Law, D. T. Umetsu, M. Conti, PDE4D plays a critical role in the control of airway smooth muscle contraction. *FASEB J* **17**, 1831-1841 (2003).
23.   C. K. Billington, I. R. Le Jeune, K. W. Young, I. P. Hall, A major functional role for phosphodiesterase 4D5 in human airway smooth muscle cells. *Am J Respir Cell Mol Biol* **38**, 1-7 (2008).
24.   A. Ray, J. K. Kolls, Neutrophilic Inflammation in Asthma and Association with Disease Severity. *Trends Immunol* **38**, 942-954 (2017).
25.   A. Butler, G. M. Walton, E. Sapey, Neutrophilic Inflammation in the Pathogenesis of Chronic Obstructive Pulmonary Disease. *COPD* **15**, 392-404 (2018).
26.   L. Abou Saleh, A. Boyd, I. V. Aragon, A. Koloteva, D. Spadafora, W. Mneimneh, R. A. Barrington, W. Richter, Ablation of PDE4B protects from Pseudomonas aeruginosa-induced acute lung injury in mice by ameliorating the cytostorm and associated hypothermia. *FASEB J* **35**, e21797 (2021).
27.   M. J. Turner, K. Abbott-Banner, D. Y. Thomas, J. W. Hanrahan, Cyclic nucleotide phosphodiesterase inhibitors as therapeutic interventions for cystic fibrosis. *Pharmacol Ther* **224**, 107826 (2021).
28.   S. D. Patel, T. R. Bono, S. M. Rowe, G. M. Solomon, CFTR targeted therapies: recent advances in cystic fibrosis and possibilities in other diseases of the airways. *Eur Respir Rev* **29**, (2020).
29.   M. J. Turner, Y. Luo, D. Y. Thomas, J. W. Hanrahan, The dual phosphodiesterase 3/4 inhibitor RPL554 stimulates rare class III and IV CFTR mutants. *Am J Physiol Lung Cell Mol Physiol* **318**, L908-L920 (2020).
30.   H. Vais, R. Zhang, W. W. Reenstra, Dibasic phosphorylation sites in the R domain of CFTR have stimulatory and inhibitory effects on channel activation. *Am J Physiol Cell Physiol* **287**, C737-745 (2004).
31.   O. Baldursson, H. A. Berger, M. J. Welsh, Contribution of R domain phosphoserines to the function of CFTR studied in Fischer rat thyroid epithelia. *Am J Physiol Lung Cell Mol Physiol* **279**, L835-841 (2000).
32.   S. Chin, M. Hung, C. E. Bear, Current insights into the role of PKA phosphorylation in CFTR channel activity and the pharmacological rescue of cystic fibrosis disease-causing mutants. *Cell Mol Life Sci* **74**, 57-66 (2017).
33.   P. D. Eckford, C. Li, M. Ramjeesingh, C. E. Bear, Cystic fibrosis transmembrane conductance regulator (CFTR) potentiator VX-770 (ivacaftor) opens the defective channel gate of mutant CFTR in a phosphorylation-dependent but ATP-independent manner. *J Biol Chem* **287**, 36639-36649 (2012).
34.   M. A. Mall, N. Mayer-Hamblett, S. M. Rowe, Cystic Fibrosis: Emergence of Highly Effective Targeted Therapeutics and Potential Clinical Implications. *Am J Respir Crit Care Med* **201**, 1193-1208 (2020).
35.   G. Veit, A. Roldan, M. A. Hancock, D. F. Da Fonte, H. Xu, M. Hussein, S. Frenkiel, E. Matouk, T. Velkov, G. L. Lukacs, Allosteric folding correction of F508del and rare CFTR mutants by elexacaftor-tezacaftor-ivacaftor (Trikafta) combination. *JCI Insight* **5**, (2020).
36.   I. d'Angelo, C. Conte, M. I. La Rotonda, A. Miro, F. Quaglia, F. Ungaro, Improving the efficacy of inhaled drugs in cystic fibrosis: challenges and emerging drug delivery strategies. *Adv Drug Deliv Rev* **75**, 92-111 (2014).
37.   C. B. Morrison, K. M. Shaffer, K. C. Araba, M. R. Markovetz, J. A. Wykoff, N. L. Quinney, S. Hao, M. F. Delion, A. L. Flen, L. C. Morton, J. Liao, D. B. Hill, M. L. Drumm, W. K. O'Neal, M. Kesimer, M. Gentzsch, C. Ehre, Treatment of cystic fibrosis airway cells with CFTR modulators reverses aberrant mucus properties via hydration. *Eur Respir J*, (2021).

38.   E. Hirsch, V. L. Katanaev, C. Garlanda, O. Azzolino, L. Pirola, L. Silengo, S. Sozzani, A. Mantovani, F. Altruda, M. P. Wymann, Central role for G protein-coupled phosphoinositide 3-kinase gamma in inflammation. *Science* **287**, 1049-1053 (2000).

39.   E. Patrucco, A. Notte, L. Barberis, G. Selvetella, A. Maffei, M. Brancaccio, S. Marengo, G. Russo, O. Azzolino, S. D. Rybalkin, L. Silengo, F. Altruda, R. Wetzker, M. P. Wymann, G. Lembo, E. Hirsch, PI3Kgamma modulates the cardiac response to chronic pressure overload by distinct kinase-dependent and -independent effects. *Cell* **118**, 375-387 (2004).

40.   L. M. DiPilato, J. Zhang, The role of membrane microdomains in shaping beta2-adrenergic receptor-mediated cAMP dynamics. *Mol Biosyst* **5**, 832-837 (2009).

41.   A. Terrin, G. Di Benedetto, V. Pertegato, Y. F. Cheung, G. Baillie, M. J. Lynch, N. Elvassore, A. Prinz, F. W. Herberg, M. D. Houslay, M. Zaccolo, PGE(1) stimulation of HEK293 cells generates multiple contiguous domains with different [cAMP]: role of compartmentalized phosphodiesterases. *J Cell Biol* **175**, 441-451 (2006).

42.   B. Ponsioen, J. Zhao, J. Riedl, F. Zwartkruis, G. van der Krogt, M. Zaccolo, W. H. Moolenaar, J. L. Bos, K. Jalink, Detecting cAMP-induced Epac activation by fluorescence resonance energy transfer: Epac as a novel cAMP indicator. *EMBO Rep* **5**, 1176-1180 (2004).

43.   W. J. Thompson, M. M. Appleman, Characterization of cyclic nucleotide phosphodiesterases of rat tissues. *J Biol Chem* **246**, 3145-3150 (1971).

44.   G. Di Benedetto, A. Zoccarato, V. Lissandron, A. Terrin, X. Li, M. D. Houslay, G. S. Baillie, M. Zaccolo, Protein kinase A type I and type II define distinct intracellular signaling compartments. *Circ Res* **103**, 836-844 (2008).

45.   R. A. Cardone, A. Bagorda, A. Bellizzi, G. Busco, L. Guerra, A. Paradiso, V. Casavola, M. Zaccolo, S. J. Reshkin, Protein kinase A gating of a pseudopodial-located RhoA/ROCK/p38/NHE1 signal module regulates invasion in breast cancer cell lines. *Mol Biol Cell* **16**, 3117-3127 (2005).

46.   K. L. Holmes, L. M. Lantz, W. Russ, Conjugation of fluorochromes to monoclonal antibodies. *Curr Protoc Cytom* **Chapter 4**, Unit 4 2 (2001).

47.   G. T. Hermanson, *Bioconjugate Techniques*. (2008).

48.   D. W. McGraw, S. L. Forbes, L. A. Kramer, D. P. Witte, C. N. Fortner, R. J. Paul, S. B. Liggett, Transgenic overexpression of beta(2)-adrenergic receptors in airway smooth muscle alters myocyte function and ablates bronchial hyperreactivity. *J Biol Chem* **274**, 32241-32247 (1999).

49.   M. Matthey, R. Roberts, A. Seidinger, A. Simon, R. Schroder, M. Kuschak, S. Annala, G. M. Konig, C. E. Muller, I. P. Hall, E. Kostenis, B. K. Fleischmann, D. Wenzel, Targeted inhibition of Gq signaling induces airway relaxation in mouse models of asthma. *Sci Transl Med* **9**, (2017).

50.   C. Laudanna, J. J. Campbell, E. C. Butcher, Role of Rho in chemoattractant-activated leukocyte adhesion through integrins. *Science* **271**, 981-983 (1996).

51.   M. Bolomini-Vittori, A. Montresor, C. Giagulli, D. Staunton, B. Rossi, M. Martinello, G. Constantin, C. Laudanna, Regulation of conformer-specific activation of the integrin LFA-1 by a chemokine-triggered Rho signaling module. *Nat Immunol* **10**, 185-194 (2009).

52.   M. Li, V. Sala, M. C. De Santis, J. Cimino, P. Cappello, N. Pianca, A. Di Bona, J. P. Margaria, M. Martini, E. Lazzarini, F. Pirozzi, L. Rossi, I. Franco, J. Bornbaum, J. Heger, S. Rohrbach, A. Perino, C. G. Tocchetti, B. H. F. Lima, M. M. Teixeira, P. E. Porporato, R. Schulz, A. Angelini, M. Sandri, P. Ameri, S. Sciarretta, R. C. P. Lima-Junior, M. Mongillo, T. Zaglia, F. Morello, F. Novelli, E. Hirsch, A. Ghigo, Phosphoinositide 3-Kinase Gamma Inhibition Protects From Anthracycline Cardiotoxicity and Reduces Tumor Growth. *Circulation* **138**, 696-711 (2018).

53.   A. Premchandar, A. Kupniewska, A. Bonna, G. Faure, T. Fraczyk, A. Roldan, B. Hoffmann, M. Faria da Cunha, H. Herrmann, G. L. Lukacs, A. Edelman, M. Dadlez, New insights into interactions between the nucleotide-binding domain of CFTR and keratin 8. *Protein Sci* **26**, 343-354 (2017).

54.   V. Montiel, R. Bella, L. Y. M. Michel, H. Esfahani, D. De Mulder, E. L. Robinson, J. P. Deglasse, M. Tiburcy, P. H. Chow, J. C. Jonas, P. Gilon, B. Steinhorn, T. Michel, C. Beauloye, L.

Bertrand, C. Farah, F. Dei Zotti, H. Debaix, C. Bouzin, D. Brusa, S. Horman, J. L. Vanoverschelde, O. Bergmann, D. Gilis, M. Rooman, A. Ghigo, S. Geninatti-Crich, A. Yool, W. H. Zimmermann, H. L. Roderick, O. Devuyst, J. L. Balligand, Inhibition of aquaporin-1 prevents myocardial remodeling by blocking the transmembrane transport of hydrogen peroxide. *Sci Transl Med* **12**, (2020).

55.   M. R. Ruggiero, S. Baroni, S. Pezzana, G. Ferrante, S. Geninatti Crich, S. Aime, Evidence for the Role of Intracellular Water Lifetime as a Tumour Biomarker Obtained by In Vivo Field-Cycling Relaxometry. *Angew Chem Int Ed Engl* **57**, 7468-7472 (2018).

56.   E. Terreno, S. Geninatti Crich, S. Belfiore, L. Biancone, C. Cabella, G. Esposito, A. D. Manazza, S. Aime, Effect of the intracellular localization of a Gd-based imaging probe on the relaxation enhancement of water protons. *Magn Reson Med* **55**, 491-497 (2006).

57.   P. Scudieri, I. Musante, E. Caci, A. Venturini, P. Morelli, C. Walter, D. Tosi, A. Palleschi, P. Martin-Vasallo, I. Sermet-Gaudelus, G. Planelles, G. Crambert, L. J. Galietta, Increased expression of ATP12A proton pump in cystic fibrosis airways. *JCI Insight* **3**, (2018).

58.   L. Zhang, M. Gallup, L. Zlock, W. E. Finkbeiner, N. A. McNamara, Rac1 and Cdc42 differentially modulate cigarette smoke-induced airway cell migration through p120-catenin-dependent and -independent pathways. *Am J Pathol* **182**, 1986-1995 (2013).

59.   M. Xie, T. C. Rich, C. Scheitrum, M. Conti, W. Richter, Inactivation of multidrug resistance proteins disrupts both cellular extrusion and intracellular degradation of cAMP. *Mol Pharmacol* **80**, 281-293 (2011).

60.   G. Veit, F. Bossard, J. Goepp, A. S. Verkman, L. J. Galietta, J. W. Hanrahan, G. L. Lukacs, Proinflammatory cytokine secretion is suppressed by TMEM16A or CFTR channel activity in human cystic fibrosis bronchial epithelia. *Mol Biol Cell* **23**, 4188-4202 (2012).

ACKNOWLEDGEMENTS

Author contributions: A. Ghigo and E.H. conceived and designed the overall study. A. Ghigo and A. Murabito. carried out the core of the experiments and analyzed the data. V.S., A.R.P and S. Bertolini performed immunoprecipitation and immunoblotting assays. A. Gianotti, E.C., W.R. and N.L.Q. performed short-circuit current measurements in Ussing chambers. A. Montresor performed all experiments with human neutrophils. A.P. performed CFTR phosphoproteomic experiments. F.P. and R.K. carried out all experiments with ovalbumin-sensitized mice. A.D.S. carried out all experiments with macrophages. M. Mergiotti, M.R.R. and S. Baroni measured water residence time. E.d.P. and S.C. carried out forskolin-induced swelling assays in organoids. M. Matthey and A.C. carried out lung function measurements. R.A.C. performed FRET-based cAMP measurements in epithelial cells. F.C. measured tracheal ring contractility. C.B. measured

PI3Kγ MP/PKA-RII dissociation constant. S.V., S.G.C., D.R., M.L., C.G.T., R.L., M.C., X.L., P.M., C.S., V.D.R, F.F., V.F., D.W., B.K.F., M.A.M., J.B., C.L., M.G., G.L.L. and N.P. provided advice on the interpretation of data. A. Ghigo, A. Murabito and E.H. wrote the manuscript with input from co-authors. All authors reviewed and approved the final manuscript.

FIGURE LEGENDS
Fig. 1. PI3Kγ decreases airway cAMP through kinase-dependent activation of PDE4B and PDE4D. (**A**) cAMP concentration in tracheas from PI3Kγ$^{+/+}$ (*n*=5), PI3Kγ$^{KD/KD}$ (*n*=5) and PI3Kγ$^{-/-}$ (*n*=4) mice. (**B**) Phosphodiesterase activity in PDE4B and PDE4D immunoprecipitates (IP) from PI3Kγ$^{+/+}$ (n=5 and n=6), PI3Kγ$^{KD/KD}$ (n=4 and n=4) and PI3Kγ$^{-/-}$ (n=5 and n=5) tracheas. Western blots of representative IPs are shown. (**C**) Phosphodiesterase activity in PDE4B and PDE4D IP from PI3Kγ$^{+/+}$ (n=8 and n=5), PI3Kγ$^{KD/KD}$ (n=4 and n=5) and PI3Kγ$^{-/-}$ (n=6 and n=5) independent cultures of murine tracheal smooth muscle cells (mTSMCs). Western blots of representative IPs are shown. (**D**) Western blot of PI3Kγ expression in mTSMCs, human bronchial smooth muscle cells (hBSMCs) and murine trachea. Peripheral blood mononuclear cells (PBMCs) are used as positive control. (**E**) Co-immunoprecipitation of PI3Kγ catalytic subunit (p110γ) with its relative adaptors (p101 and p84/87) and PKA catalytic subunit (PKA-C) in hBSMCs. (**F**) Co-immunoprecipitation of PI3Kγ with PDE4B and PDE4D in hBSMCs. IgG immunoprecipitation was used as control. In (**D**), (**E**) and (**F**), representative Western blot images of *n*=4 independent experiments are shown. (**G**) (Left) Representative fluorescence resonance energy transfer (FRET) traces and (right) maximal FRET changes (Max ΔFRET) of hBSMCs transfected with a FRET–based sensor for cytosolic cAMP (Epac2-cAMPs), together with either an shRNA against the *PIK3CG* gene encoding PI3Kγ (PI3Kγ shRNA; n=7) or a

scrambled shRNA (scr shRNA; n=9) vector. β_2-ARs were selectively activated by isoproterenol (Iso; 100 nmol/L, 15 seconds) and the β_1-AR selective antagonist CGP-20712A (CGP; 100 nmol/L). Insets, representative cyan and yellow fluorescence protein images of hBSMCs expressing Epac2-cAMPs. *n* indicates the number of cells analyzed in *n*=3 independent experiments. Representative Western blot of PI3Kγ expression in hBSMCs 48 hours after transfection with the PI3Kγ shRNA and scr shRNA is shown below the graph. In (**A**), (**B**) and (**C**), *P<0.05, **P<0.01 and ***P<0.001 by one-way ANOVA followed by Bonferroni's post-hoc test. In (**G**), **P<0.01 by Mann-Whitney test. Throughout, data are mean ± SEM.

Fig. 2. PI3Kγ MP enhances airway β_2-AR/cAMP signaling in vitro. (**A**) Top, schematic representation of the cell-permeable PI3Kγ mimetic peptide (PI3Kγ MP). The 126-150 region of PI3Kγ was fused to the cell-penetrating peptide penetratin 1 (P1). Bottom, intracellular fluorescence of human bronchial smooth muscle cells (hBSMCs) following 1 hour incubation with a FITC-labeled version of PI3Kγ MP (50 µM) or vehicle. Scale bar: 10 µm. (**B**) Steady-state emission spectra of recombinant fluorescein 5-maleimide-labelled PKA-RII (PKA-F5M) in the presence of increasing concentrations of PI3Kγ MP (0-150 µM), revealing a dissociation constant for PI3Kγ MP/PKA-RII interaction of 7.5 µM. (**C**) Co-immunoprecipitation of the catalytic subunit of PI3Kγ (p110γ) and PKA-RII from HEK-293T cells expressing p110γ and exposed to increasing doses of PI3Kγ MP for 2 hours. Representative immunoblots (left) and relative quantification (right) of *n*=3 independent experiments are shown. (**D**) PDE4B and PDE4D activity in PI3K$\gamma^{+/+}$ and PI3K$\gamma^{-/-}$ mouse tracheal smooth muscle cells (mTSMCs) treated with either vehicle (Veh) or PI3Kγ MP (50 µM) for 30 min. For PDE4B IP: PI3K$\gamma^{+/+}$+Veh n=4; PI3K$\gamma^{+/+}$+PI3Kγ MP n=5; PI3K$\gamma^{-/-}$+Veh n=5 and PI3K$\gamma^{-/-}$+ PI3Kγ MP n=5 independent cultures. For PDE4D IP: n=3 independent cultures in all groups. (**E**) Representative FRET traces (left) and maximal FRET changes (right) in human tracheal smooth muscle cells (hBSMCs) expressing the ICUE3 cAMP FRET sensor and pre-treated for 30 min with vehicle (n=9), 50 µM PI3Kγ MP (n=6) or equimolar control peptide (CP; n=11) before activation of β_2-adrenergic receptors (β_2-ARs) with isoproterenol and the β_1-AR antagonist CGP-20712A (Iso + CGP; 100 nM each). Insets show representative intensity-modulated pseudocolor images at t = 0 s and 500 s after the addition of Iso+CGP. n indicates the number of cells analysed in n=3 independent experiments. (**F**) cAMP elevation in human bronchial epithelial cells (16HBE14o-) in response to increasing concentrations of PI3Kγ MP (31.6 nM – 316 µM range) for 30 min. The amount of cAMP was expressed as percentage of cAMP accumulation elicited by 100 µM PI3Kγ MP. N=6 independent experiments. In (**C**), (**D**) and €, *P<0.05, **P<0.01, ***P<0.001 by one-way ANOVA followed by Bonferroni's post-hoc test. In (**F**), non-linear regression analysis was used. Throughout, data are mean ± SEM.

Fig. 3. PI3Kγ MP elevates airway cAMP abundance in vivo in mice. (**A**) cAMP concentrations in tissues from BALB/c mice 24 hours after intratracheal instillation of different doses of PI3Kγ MP (0-750 µg/kg). Values in brackets indicate the dose of PI3Kγ MP expressed as µg/kg. The number of mice (n) ranged from 3 to 9 per group. (**B**) Tissue distribution of a FITC-labeled version of PI3Kγ MP at indicated time points after intratracheal instillation of 0.08 mg/kg (1.5 µg) in BALB/c mice. Representative images of n=3 experiments are shown. Scale bar: 50 µm. (**C**) Amount of cAMP in tissues from mice treated as in (**B**). The number of mice (n) ranged from 3 to 6 per group. In (**A**), *P<0.05, **P<0.01, ***P<0.001 by one-way ANOVA

followed by Bonferroni's post-hoc test. In (**C**), *P<0.05 by Kruskal Wallis test followed by Dunn's multiple comparison test. Throughout, data are mean ± s.e.m.

Fig. 4. PI3Kγ MP promotes airway relaxation ex vivo and in vivo in a mouse model of asthma. (**A** and **B**) Cumulative contractile response of PI3Kγ$^{+/+}$, PI3Kγ$^{KD/KD}$ and PI3Kγ$^{-/-}$ tracheal rings to increasing concentrations of acetylcholine (**A**) and carbachol (**B**). The developed tension is expressed as a percentage of the resting tone. In (**A**), PI3Kγ$^{+/+}$ n=7, PI3Kγ$^{KD/KD}$ n=6 and PI3Kγ$^{-/-}$ n=5 mice. In (**B**), PI3Kγ$^{+/+}$ n=9, PI3Kγ$^{KD/KD}$ n=6 and PI3Kγ$^{-/-}$ n=5 mice. (**C**) Cumulative contractile response to carbachol of PI3Kγ$^{+/+}$ and PI3Kγ$^{-/-}$ tracheal rings pre-treated with either vehicle (Veh) or the PDE4 inhibitor Roflumilast (Ro, 10 µM) for 30 min. PI3Kγ$^{+/+}$+Veh n=10, PI3Kγ$^{+/+}$+Ro n=5, PI3Kγ$^{-/-}$+Veh n=13, and PI3Kγ$^{-/-}$+Ro n=9 mice. (**D**) Average lung resistance in healthy mice treated with vehicle (n=4), 1.5 µg PI3Kγ MP (n=4) or equimolar amount of control peptide (CP; n=5) directly before exposure to increasing doses of the bronchoconstrictor methacholine (MCh). (**E**) cAMP concentrations in lungs and tracheas of ovalbumin (OVA)-sensitized mice at the indicated time points after intra-tracheal administration of PI3Kγ MP (15 µg). The number of mice (n) ranged from 3 to 8 per group. (**F**) Tidal volume of ovalbumin (OVA)-sensitized mice pre-treated with vehicle (n=5), PI3Kγ MP (15 µg; n=6) and CP (equimolar amounts; n=5) and exposed to methacholine (MCh; 500 µg/kg). (**G**) Average lung resistance (expressed as % of basal) in OVA-sensitized mice treated with 15 µg of PI3Kγ MP (n=9) or equimolar amount of CP (n=10) 30 min before methacholine challenge. In (**A**) and (**B**), *P<0.05, **P<0.01 and ***P<0.001 versus PI3Kγ$^{+/+}$ and #P<0.05 and ##P<0.01 versus PI3Kγ$^{KD/KD}$ by two-way ANOVA followed by Bonferroni's multiple comparisons test. In (**C**), **P<0.01 and ***P<0.001 for PI3Kγ$^{+/+}$+Veh versus all other groups by two-way ANOVA followed by Bonferroni's multiple comparisons test. In (**D**), **P<0.01 and ***P<0.001 versus vehicle and ### P<0.001 versus CP by two-way ANOVA followed by Bonferroni's post-hoc test. In (**E**) and (**F**), *P<0.05 and **P<0.01 by one-way ANOVA followed by Bonferroni's post-hoc test. In (**G**), *P<0.05 and **P<0.01 between groups by two-way ANOVA followed by Bonferroni's post-hoc test. Throughout, data are mean ± SEM.

Fig. 5. PI3Kγ MP limits neutrophilic lung inflammation in asthmatic mice. (**A**) Representative images of hematoxylin-eosin (top) and periodic acid-Schiff's reagent (bottom) staining of lung sections of naïve and ovalbumin (OVA)-sensitized mice, pre-treated with PI3Kγ MP (25 µg) or CP (equimolar amount), before each intranasal OVA administration (days 14, 25, 26 and 27 of the OVA sensitization protocol). Scale bar: 50 µm. (**B**) Semi-quantitative analysis of peribronchial inflammation in lung sections as shown in (**A**). Naïve n=6, OVA+CP n=8 and OVA+PI3Kγ MP n=5 mice. (**C**) Number of neutrophils (NΦ), eosinophils (EΦ), lymphocytes (LΦ) and macrophages (MΦ) in the bronchoalveolar lavage (BAL) fluid of mice treated as in (**A**). Naïve n=3, OVA+CP n=8 and OVA+PI3Kγ MP n=5 animals. (**D** to **F**) fMLP-induced adhesion to ICAM-1 (**D**), ICAM-2 (**E**) and fibrinogen (**F**) of human neutrophils pre-treated or not with the PKA inhibitor H89 (200 nM, 30 min) before exposure to vehicle or PI3Kγ MP (50 µM, 1 hour). Static adhesion was induced with 25 nM fMLP for 1 min. Average numbers of adherent cells/0.2 mm^2 is shown. In (**D**) and (**F**), n=3 in all groups; in (**E**), n=4 in all groups. (**G**) fMLP-triggered chemotaxis of human neutrophils treated with vehicle, CP (50 µM) or PI3Kγ MP (50 µM) for 1 hour, without or with pre-treatment with the PKA inhibitor H89 (200 nM, 30 min). n=4 in all groups. (**G**) fMLP-induced RhoA activity in human neutrophils treated with vehicle, CP (50 µM) or PI3Kγ MP (50 µM). n=3 in all groups. In (**B**), **P<0.01 and ***P

<0.001 by Kruskal Wallis test followed by Dunn's multiple comparison test. In (**C**), (**D**), (**E**), (**F**), (**G**) and (**H**), *P <0.05, **P<0.01 and ***P <0.001 by one-way ANOVA followed by Bonferroni's post-hoc test.

Fig. 6. PI3Kγ MP promotes cAMP-dependent gating of CFTR. (**A**) Representative FRET traces (left) and maximal FRET changes (right) in human bronchial epithelial cells (16HBE14o-) expressing the FRET probe for either plasma membrane (pm cAMP) or cytosolic cAMP (cyt cAMP). Cells were pre-incubated with vehicle (Veh), PI3Kγ MP (25 µM) or control peptide (CP; 25 µM) before treatment with 1 µM forskolin (Fsk). R is the normalized 480 nm/545nm emission ratio calculated at indicated time points. n indicates number of cells from n=3 independent experiments. Veh n=10 and n=12, PI3Kγ MP n=22 and n=11, CP n=3 and n=7, for pm cAMP and cyt cAMP, respectively. (**B**) Representative Western blot (left) and relative quantification (right) of PKA-mediated phosphorylation of CFTR in 16HBE14o- cells treated with vehicle, CP (25 µM), PI3Kγ MP (25 µM) and the PDE4 inhibitor Rolipram (PDE4i; 10 µM) for 30 min. CFTR was immunoprecipitated (IP) and PKA-dependent phosphorylation was detected in IP pellets by immunoblotting with a PKA substrate antibody. n=4 independent experiments. (**C**) Relative phosphorylation (%) or phospho-occupancy of identified PKA sites of CFTR in wt-CFTR-CFBE41o- expressing HBH-CFTR-3HA treated with vehicle (DMSO; n=7), PI3Kγ MP (25 µM, 1 hour, n=3) and Fsk (10 µM, 10 min, n=7). n is the number of biological replicates from n=3 independent experiments. The phospho-occupancy or the percent of relative phosphorylation of each site was calculated as a ratio of all phosphorylated and unphosphorylated peptides that contained a given phosphorylation site (% phosphorylation of site A = [area of peptides phosphorylated at site A /sum of areas of all peptides carrying site A] as described in Methods). Representative fragmentation spectra from each identified phosphorylation site and representative chromatograms from S737-containing peptides in their unphosphorylated and phosphorylated form are provided in Fig. S6. (**D**) Representative Western blot (left) and relative quantification (right) of PKA-mediated phosphorylation of CFTR in HEK293T cells expressing either wt- or S737A-CFTR and exposed to vehicle, PI3Kγ MP (25 µM, 1 hour) or Fsk (10 µM, 10 min). n=4 independent experiments. (**E**) left, Representative trace of short-circuit currents (I_{SC}) measured in Ussing chambers in primary human normal bronchial epithelial (HBE) cells cultured at the air-liquid interface (ALI). The following treatments were applied at the indicated times: ENaC inhibitor amiloride (10 µM), CP (30 µM), PI3Kγ MP (10-30 µM), PDE4 inhibitor Rolipram (PDE4i; 10 µM), forskolin (Fsk, 10 µM) and CFTR inhibitor 172 (CFTR$_{inh}$-172; 20 µM). Right, average current variations in response to the indicated treatments. n=3 biological replicates from the same donor. (**F**) Normalized swelling curves (left) and representative confocal images (right) of Fsk-stimulated calcein green-labeled wild-type (wt) organoids pre-incubated with PI3Kγ MP (25 µM) or vehicle (Veh) for 20 min. Fsk was used at 2 µM. Scale bar: 100 µm. Veh n=25 and PI3Kγ MP n=28 organoids from n=3 independent experiments. (**G**) Water residence time (τ_{in}) determined by 1H NMR relaxometry (as described in Supplementary Material) in HEK293T cells transfected with wt-CFTR and treated with vehicle (DMSO; n=8), CP (25 µM; n=3) and PI3Kγ MP (25 µM; n=11). n indicates the number of biological replicates in n=3 independent experiments. In (**A**), (**B**), (**D**), (**E**) and (**G**), *P<0.05, **P <0.01 and ***P <0.001 by one-way ANOVA followed by Bonferroni's post-hoc test. In (**C**), unpaired t-tests followed by Holm-Sidak's multiple comparisons test were performed on each phosphorylation site between two different treatment conditions. #P<0.05, ##P <0.01 and ###P<0.001 Fsk versus vehicle, *P<0,05 PI3Kγ MP versus vehicle. (**F**) *P<0.05 and

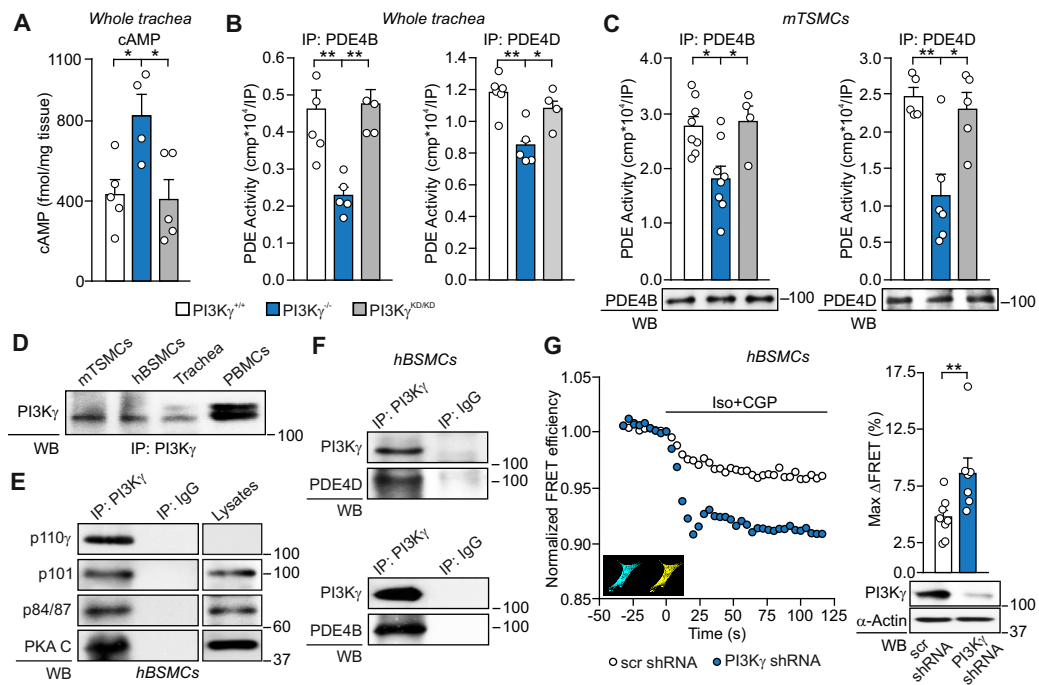***P<0.001 by two-way ANOVA followed by Bonferroni's multiple comparisons test. Throughout, data are mean ± SEM.

Fig. 7. PI3Kγ MP potentiates the therapeutic effects of CFTR modulators in CF in vitro models. (**A**) Representative FRET traces (left) and maximal FRET changes (right) in CFBE41o-cells overexpressing F508del-CFTR and the plasma membrane-targeted FRET probe for cAMP (pm cAMP). Cells were pre-incubated with vehicle (Veh), the CFTR corrector VX-809 (5 µM) alone or together with PI3Kγ MP (25 µM) before treatment with 1 µM Fsk. R is the normalized 480 nm/545nm emission ratio calculated at indicated time points. Veh n=12, VX-809 n=22 and VX-809+PI3Kγ MP n=16 where n is the number of cells from n=3 independent experiments. (**B**) Left, Representative trace of short-circuit currents (I_{SC}) in primary human bronchial epithelial cells from a donor with CF (Patient #1) homozygous for the F508del mutation (F508del/F508del HBE) and grown at the air-liquid interface (ALI). Cells were corrected with VX-809 for 48 hours (5 µM) and then exposed to the following drugs at the indicated times: Amiloride (Amil, 100 µM), CP (10 µM), PI3Kγ MP (10 µM), forskolin (Fsk, 10 µM), VX-770 (1 µM) and the CFTR inhibitor 172 (CFTR_inh-172; 10 µM). Right, Average total current variation in response to VX-770 (1 µM), CP (10 µM), PI3Kγ MP (10 µM) and forskolin (Fsk, 10 µM) of n=4 technical replicates of the same donor. (**C**) Average total current variation in response to VX-770 (1 µM), CP (25 µM) and PI3Kγ MP (25 µM) in F508del/F508del HBE cells from a second donor with CF (Patient #2) grown at ALI and pre-corrected with VX-809 for 48 hours (5 µM). n=4 technical replicates of the same donor. Representative I_{SC} traces are provided in Fig. S9A-C. (**D**) Representative confocal images and forskolin-induced swelling (FIS) of calcein green-labeled rectal organoids from a patient carrying compound CF F508del and D1152H mutations (F508del/D1152H). Organoids were corrected with VX-809 (3 µM) for 24 hours, incubated with calcein-green (3 µM) for 30 min and exposed to either PI3Kγ MP or CP (both 25 µM) for 30 min before stimulation with Fsk (2 µM). Organoid response was measured as percentage change in volume at different time points after addition of Fsk (t=30, t=60, and t=120 min) compared to the volume at t=0. n=15-34 organoids from 1 donor in n=2 independent experiments. Scale bar: 200 µm. (**E**) FIS responses (right) and representative confocal images (left) of calcein green-labeled rectal organoids from a CF patient homozygous for the F508del mutation (F508del/F508del). Organoids were pre-incubated with the CFTR corrector VX-809 (3 µM) and the CFTR potentiator VX-770 (3 µM) for 24 hours before exposure to two different concentrations of Fsk (0.51 µM; 0.128 µM) and PI3Kγ MP (10 µM; 25 µM). The peptide was added to the organoids together with Fsk. Organoid response was measured as area under the curve of relative size increase of organoids after 60 min Fsk stimulation, t = 0 min: baseline of 100%. n=12 organoids/group analyzed in n=2 independent cultures from n=2 different donors. Scale bar: 200 µm. In (**A**), (**B**), and (**C**), **P <0.01 and ***P <0.001 by one-way ANOVA followed by Bonferroni's post-hoc test. In (**D**), *P<0.05 and ***P<0.001 by two-way ANOVA followed by Bonferroni's post-hoc test. In (**E**), ***P <0.001 by Kruskal Wallis test followed by Dunn's multiple comparison test. Throughout, data are mean ± SEM

Fig. 8. PI3Kγ MP enhances the effect of elexacaftor/tezacaftor/ivacaftor in primary F508del/F508del HBE cells. (**A**) Representative traces of I_{SC} in primary human CF bronchial epithelial cells from a donor with CF (Patient BE93) homozygous for the F508del mutation (F508del/F508del HBE) and grown at the air-liquid interface (ALI). Cells were corrected for 24 hours with VX-661 and VX-445 alone (10µM+3µM) or together with PI3Kγ MP (10 µM),

before exposure at the indicated time to the following drugs: Amiloride (100 µM), VX-770 (1 µM), CPT-cAMP (100 µM), and CFTR$_{inh}$-172 (10 µM). (**B**) Average total current variation in response to VX-770 (1 µM) from n=5-8 technical replicates of donor BE93. (**C**) Average total current variation in response to VX-770 (1 µM) from n=5 technical replicates of a second F508del/F508del donor (patient BE91). Representative I$_{SC}$ traces are provided in Fig. S9E. Throughout, *P<0.05 and **P<0.001 and by Student's *t* test. Data are mean ± SEM.

A *Whole trachea*
cAMP

B *Whole trachea*
IP: PDE4B   IP: PDE4D

C *mTSMCs*
IP: PDE4B   IP: PDE4D

PDE4B   —100
WB

PDE4D   —100
WB

□ PI3Kγ$^{+/+}$ ■ PI3Kγ$^{-/-}$ ▨ PI3Kγ$^{KD/KD}$

D
mTSMCs hBSMCs Trachea PBMCs
PI3Kγ   —100
WB   IP: PI3Kγ

E
IP: PI3Kγ   IP: IgG   Lysates
p110γ   —100
p101   —100
p84/87   —60
PKA C   —37
WB   *hBSMCs*

F *hBSMCs*
IP: PI3Kγ   IP: IgG
PI3Kγ   —100
PDE4D   —100
WB

IP: PI3Kγ   IP: IgG
PI3Kγ   —100
PDE4B   —100
WB

G *hBSMCs*
Iso+CGP

Max ΔFRET (%)

PI3Kγ   —100
α-Actin   —37
WB   scr   PI3Kγ
     shRNA shRNA

○ scr shRNA   ● PI3Kγ shRNA

A PI3Kγ mimetic peptide (MP)

Penetratin 1 | PI3Kγ aa 126-150

KATHRSPGQIHLVQRHPPSEESQAF

Vehicle

PI3Kγ MP

FITC peptide/Actin/DAPI
hBSMCs

B

Intensity (AU)

K_b=7.5 µM

PI3Kγ MP (µM)
0
0.01
0.1
1
10
20
50
100
150

Wavelength (nm)

Intensity (AU)

Wavelength (nm)

C

PI3Kγ/PKA-RII ratio

HEK293T

PI3Kγ MP (µM)

0   1   25   50

p110γ
PKA-C
WB

Control peptide (µM)

0   1   25   50

p110γ
PKA-C
WB   IP:PKA-RII

p110γ bound to PKA-RII (AU)

PI3Kγ MP   0   1   25   50   µM

D *mTSMCs*

IP: PDE4B

PDE Activity (cpm*10³/IP)

PI3Kγ MP   -   +   -   +

IP: PDE4D

PDE Activity (cpm*10⁴/IP)

PI3Kγ MP   -   +   -   +

☐ PI3Kγ⁺/⁺   ■ PI3Kγ⁻/⁻

E

Vehicle   PI3Kγ MP   CP

t = 0s

t = 500s

FRET efficiency

☐ Vehicle
■ PI3Kγ MP
▨ CP

Apparent FRET efficiency (normalized)

Iso+CGP

○ Vehicle
◐ CP
● PI3Kγ MP

hBSMCs

Time (s)

Max ΔFRET (%)

F

cAMP concentration (% of maximal response)

EC₅₀=21.66 µM

16HBE14o-

PI3Kγ MP (LogM)

A

Trachea

cAMP (pmol/mg) vs PI3Kγ MP (log μg/Kg)

** (25), *** (80), *** (250), *** (750)

(2.5) (8.5) EC$_{50}$=13.9 μg/Kg

Lungs

cAMP (pmol/mg) vs PI3Kγ MP (log μg/Kg)

* (80), ** (250), * (750)

(2.5) (8.5) (25) EC$_{50}$=13.5 μg/Kg

Hearts

cAMP (pmol/mg) vs PI3Kγ MP (log μg/Kg)

(2.5) (8.5) (25) (80) (250) (750)

B

0 | 2 hours | 1day | 4 days

Lungs

Trachea

Hearts

C

Trachea

cAMP (pmol/mg) vs Hours after PI3Kγ MP

* (24)

Lungs

cAMP (pmol/mg) vs Hours after PI3Kγ MP

* (24)

Hearts

cAMP (pmol/mg) vs Hours after PI3Kγ MP

A

Naive | OVA + CP | OVA+ PI3Kγ MP

H&E

PAS

B

□ Naive
■ OVA + CP
■ OVA + PI3Kγ MP

Inflammatory index in the lung

*** **

C

□ Naive
■ OVA + CP
■ OVA + PI3Kγ MP

10⁴ cells/ml

** *
* *

NΦ   EΦ   LΦ   MΦ

D *Adhesion ICAM-1*

NΦ adherent to ICAM-1

*** ***

Ut   fMLP

E *Adhesion ICAM-2*

NΦ adherent to ICAM-2

*** ns

Ut   fMLP

F *Adhesion Fibrinogen*

NΦ adherent to fibrinogen

** ns

Ut   fMLP

G *Chemotaxis*

Migrated NΦ x10⁵/1h

*** ***

Ut   fMLP

H *RhoA activity*

RhoA activation (O.D. 490 nm)

*** ***

Ut   fMLP

□ Vehicle   ■ CP   ■ PI3Kγ MP   ▧ H89   ▨ H89 + PI3Kγ MP

A

pm cAMP

R (480/545 nm)

○ Vehicle
● PI3Kγ MP
○ CP

Fsk

16HBE41o-

Time (s)

cyt cAMP

R (480/545 nm)

○ Vehicle
● PI3Kγ MP
○ CP

Fsk

Time (s)

cAMP distribution

cAMP distribution ($\Delta R/R_0$ %)

□ Vehicle
■ PI3Kγ MP
■ CP

*** ***

plasma membrane   cytosol

B

16HBE14o-

PI3Kγ MP	−	−	+	−
CP	−	+	−	−
PDE4i	−	−	−	+

P-PKA Substrate — 150

CFTR — 150

WB   IP:CFTR

PKA phosphorylation of CFTR

Phospho-CFTR (AU)

***
***

Ctrl CP MP PDE4i

C

HBH-CFTR-3HA-CFBE41o-

% CFTR Phosphorylation

□ Vehicle
■ PI3Kγ MP
■ Fsk

##
    ###   ##   * ##
                                    *

S422 S660 S670 S686 S700 S712 S737 S753 S768 S795

D

HEK293T

wt-CFTR	+	+	+	−	−	+	−
S737A-CFTR	+	−	−	+	+	−	+
PI3Kγ MP	−	−	+	−	+	−	−
FSK	−	−	−	−	−	+	+

P-PKA Substrate — 150

CFTR — 150

WB   IP: IgG   IP:CFTR

PKA phosphorylation of CFTR

Phospho-CFTR (AU)

□ Vehicle
■ PI3Kγ MP

*

wt   S737A

E

CFTR$_{inh}$-172

Fsk

PI3Kγ MP 30 μM

PI3Kγ MP 20 μM

PDE4i

PI3Kγ MP 10 μM

Amiloride

CP

4 μA/cm²

2 min

HBE cells

ΔI_{sc} (μA/cm²)

***
**
**

Ctrl 10 20 30 Fsk
PI3Kγ MP (μM)

F

wt organoids

Organoid volume (%)

○ Vehicle
● PI3Kγ MP

Fsk

*** *** ***
*

Time (min)

Vehicle

PI3Kγ MP

0 min   30 min

G

HEK293T

Intracellular water lifetime (s)

□ Veh
■ CP
■ PI3Kγ MP

*** ***

Veh CP PI3Kγ MP

A *pm cAMP*

R (480/545 nm) vs Time (s)
○ Vehicle
● VX-809
● VX-809+PI3Kγ MP
Fsk

F508del-CFTR-CFBE41o-

cAMP (ΔR/R₀ %)
** ***
Vehicle ■ VX-809 ■ VX-809+PI3Kγ MP

B *VX-809-corrected*

CFTRinh-172
PI3Kγ MP 10 μM
Fsk
Amiloride
VX-770
CP
3 μA/cm²
2 min
F508del/F508del HBE

Patient #1
ΔIsc (μA/cm²)
**

VX-770	+	+	+	+
CP	-	+	-	-
PI3Kγ MP	-	-	+	-
Fsk	-	-	-	+

C *Patient #2*
ΔIsc (μA/cm²)
***

VX-770	+	+	+
CP	-	+	-
PI3Kγ MP	-	-	+

D
0 min   60 min
CP
PI3Kγ MP
PI3Kγ MP+CFTRinh-172

F508del/D1152H organoids
Normalized organoids volume (%)
Fsk
VX-770
MP or CP
***
*
***
***
VX-809-corrected
Time (min)
● CP ● PI3Kγ MP ○ PI3Kγ MP+CFTRinh-172

E
0 min   60 min
Vehicle
VX-809+VX-770
PI3Kγ MP (10)
PI3Kγ MP (25)

F508del/F508del organoids
AUC at t= 60 min
6.5x
*** ***
PI3Kγ MP (μM)   0   10   25
□ 0.051 μM Fsk
▨ 0.128 μM Fsk

A

chronic VX-661 + VX-445

Amiloride

VX-770   CPTcAMP   CFTR$_{inh}$-172

10 µA/cm^2

10 min

chronic VX-661 + VX-445 + PI3Kγ MP

Amiloride

CPTcAMP   CFTR$_{inh}$-172

VX-770

10 µA/cm^2

10 min

Patient BE93
F508del/F508del HBE

B   *Patient BE93*

CFTR-mediated current
elicited by VX-770 (mA/cm^2)

12

9

6

3

0

**

C   *Patient BE91*

CFTR-mediated current
elicited by VX-770 (mA/cm^2)

10

8

6

4

2

0

*

VX-661+VX-445+VX-770

VX-661+VX-445+VX-770 +PI3Kγ MP